

Measurement of the $t\bar{t}$ Production Cross Section in $p\bar{p}$ Collisions at $\sqrt{s} = 1.96$ TeV using Missing E_T +jets Events with Secondary Vertex b -Tagging

- A. Abulencia,²³ D. Acosta,¹⁷ J. Adelman,¹³ T. Affolder,¹⁰ T. Akimoto,⁵³ M.G. Albrow,¹⁶ D. Ambrose,¹⁶ S. Amerio,⁴² D. Amidei,³³ A. Anastassov,⁵⁰ K. Anikeev,¹⁶ A. Annovi,⁴⁴ J. Antos,¹ M. Aoki,⁵³ G. Apollinari,¹⁶ J.-F. Arguin,³² T. Arisawa,⁵⁵ A. Artikov,¹⁴ W. Ashmanskas,¹⁶ A. Attal,⁸ F. Azfar,⁴¹ P. Azzi-Bacchetta,⁴² P. Azzurri,⁴⁴ N. Bacchetta,⁴² H. Bachacou,²⁸ W. Badgett,¹⁶ A. Barbaro-Galtieri,²⁸ V.E. Barnes,⁴⁶ B.A. Barnett,²⁴ S. Baroiant,⁷ V. Bartsch,³⁰ G. Bauer,³¹ F. Bedeschi,⁴⁴ S. Behari,²⁴ S. Belforte,⁵² G. Bellettini,⁴⁴ J. Bellinger,⁵⁷ A. Belloni,³¹ E. Ben-Haim,¹⁶ D. Benjamin,¹⁵ A. Beretvas,¹⁶ J. Beringer,²⁸ T. Berry,²⁹ A. Bhatti,⁴⁸ M. Binkley,¹⁶ D. Bisello,⁴² M. Bishai,¹⁶ R. E. Blair,² C. Blocker,⁶ K. Bloom,³³ B. Blumenfeld,²⁴ A. Bocci,⁴⁸ A. Bodek,⁴⁷ V. Boisvert,⁴⁷ G. Bolla,⁴⁶ A. Bolshov,³¹ D. Bortoletto,⁴⁶ J. Boudreau,⁴⁵ S. Bourov,¹⁶ A. Boveia,¹⁰ B. Brau,¹⁰ C. Bromberg,³⁴ E. Brubaker,¹³ J. Budagov,¹⁴ H.S. Budd,⁴⁷ S. Budd,²³ K. Burkett,¹⁶ G. Busetto,⁴² P. Bussey,²⁰ K. L. Byrum,² S. Cabrera,¹⁵ M. Campanelli,¹⁹ M. Campbell,³³ F. Canelli,⁸ A. Canepa,⁴⁶ D. Carlsmith,⁵⁷ R. Carosi,⁴⁴ S. Carron,¹⁵ M. Casarsa,⁵² A. Castro,⁵ P. Catastini,⁴⁴ D. Cauz,⁵² M. Cavalli-Sforza,³ A. Cerri,²⁸ L. Cerrito,⁴¹ S.H. Chang,²⁷ J. Chapman,³³ Y.C. Chen,¹ M. Chertok,⁷ G. Chiarelli,⁴⁴ G. Chlachidze,¹⁴ F. Chlebana,¹⁶ I. Cho,²⁷ K. Cho,²⁷ D. Chokheli,¹⁴ J.P. Chou,²¹ P.H. Chu,²³ S.H. Chuang,⁵⁷ K. Chung,¹² W.H. Chung,⁵⁷ Y.S. Chung,⁴⁷ M. Ciljak,⁴⁴ C.I. Ciobanu,²³ M.A. Ciocci,⁴⁴ A. Clark,¹⁹ D. Clark,⁶ M. Coca,¹⁵ A. Connolly,²⁸ M.E. Convery,⁴⁸ J. Conway,⁷ B. Cooper,³⁰ K. Copic,³³ M. Cordelli,¹⁸ G. Cortiana,⁴² A. Cruz,¹⁷ J. Cuevas,¹¹ R. Culbertson,¹⁶ D. Cyr,⁵⁷ S. DaRonco,⁴² S. D'Auria,²⁰ M. D'onofrio,¹⁹ D. Dagenhart,⁶ P. de Barbaro,⁴⁷ S. De Cecco,⁴⁹ A. Deisher,²⁸ G. De Lentdecker,⁴⁷ M. Dell'Orso,⁴⁴ S. Demers,⁴⁷ L. Demortier,⁴⁸ J. Deng,¹⁵ M. Deninno,⁵ D. De Pedis,⁴⁹ P.F. Derwent,¹⁶ C. Dionisi,⁴⁹ J.R. Dittmann,⁴ P. DiTuro,⁵⁰ C. Dörr,²⁵ A. Dominguez,²⁸ S. Donati,⁴⁴ M. Donega,¹⁹ P. Dong,⁸ J. Donini,⁴² T. Dorigo,⁴² S. Dube,⁵⁰ K. Ebina,⁵⁵ J. Efron,³⁸ J. Ehlers,¹⁹ R. Erbacher,⁷ D. Errede,²³ S. Errede,²³ R. Eusebi,⁴⁷ H.C. Fang,²⁸ S. Farrington,²⁹ I. Fedorko,⁴⁴ W.T. Fedorko,¹³ R.G. Feild,⁵⁸ M. Feindt,²⁵ J.P. Fernandez,⁴⁶ R. Field,¹⁷ G. Flanagan,³⁴ L.R. Flores-Castillo,⁴⁵ A. Foland,²¹ S. Forrester,⁷ G.W. Foster,¹⁶ M. Franklin,²¹ J.C. Freeman,²⁸ Y. Fujii,²⁶ I. Furic,¹³ A. Gajjar,²⁹ M. Gallinaro,⁴⁸ J. Galyardt,¹² J.E. Garcia,⁴⁴ M. Garcia Sciveres,²⁸ A.F. Garfinkel,⁴⁶ C. Gay,⁵⁸ H. Gerberich,²³ E. Gerchtein,¹² D. Gerdes,³³ S. Giagu,⁴⁹ P. Giannetti,⁴⁴ A. Gibson,²⁸ K. Gibson,¹² C. Ginsburg,¹⁶ K. Giolo,⁴⁶ M. Giordani,⁵² M. Giunta,⁴⁴ G. Giurgiu,¹² V. Glagolev,¹⁴ D. Glenzinski,¹⁶ M. Gold,³⁶ N. Goldschmidt,³³ J. Goldstein,⁴¹ G. Gomez,¹¹ G. Gomez-Ceballos,¹¹ M. Goncharov,⁵¹ O. González,⁴⁶ I. Gorelov,³⁶ A.T. Goshaw,¹⁵ Y. Gotra,⁴⁵ K. Goulianatos,⁴⁸ A. Gresele,⁴² M. Griffiths,²⁹ S. Grinstein,²¹ C. Grossos-Pilcher,¹³ U. Grundler,²³ J. Guimaraes da Costa,²¹ C. Haber,²⁸ S.R. Hahn,¹⁶ K. Hahn,⁴³ E. Halkiadakis,⁴⁷ A. Hamilton,³² B.-Y. Han,⁴⁷ R. Handler,⁵⁷ F. Happacher,¹⁸ K. Hara,⁵³ M. Hare,⁵⁴ S. Harper,⁴¹ R.F. Harr,⁵⁶ R.M. Harris,¹⁶ K. Hatakeyama,⁴⁸ J. Hauser,⁸ C. Hays,¹⁵ H. Hayward,²⁹ A. Heijboer,⁴³ B. Heinemann,²⁹ J. Heinrich,⁴³ M. Hennecke,²⁵ M. Herndon,⁵⁷ J. Heuser,²⁵ D. Hidas,¹⁵ C.S. Hill,¹⁰ D. Hirschbuehl,²⁵ A. Hocker,¹⁶ A. Holloway,²¹ S. Hou,¹ M. Houlden,²⁹ S.-C. Hsu,⁹ B.T. Huffman,⁴¹ R.E. Hughes,³⁸ J. Huston,³⁴ K. Ikado,⁵⁵ J. Incandela,¹⁰ G. Introzzi,⁴⁴ M. Iori,⁴⁹ Y. Ishizawa,⁵³ A. Ivanov,⁷ B. Iyutin,³¹ E. James,¹⁶ D. Jang,⁵⁰ B. Jayatilaka,³³ D. Jeans,⁴⁹ H. Jensen,¹⁶ E.J. Jeon,²⁷ M. Jones,⁴⁶ K.K. Joo,²⁷ S.Y. Jun,¹² T.R. Junk,²³ T. Kamon,⁵¹ J. Kang,³³ M. Karagoz-Unel,³⁷ P.E. Karchin,⁵⁶ Y. Kato,⁴⁰ Y. Kemp,²⁵ R. Kephart,¹⁶ U. Kerzel,²⁵ V. Khotilovich,⁵¹ B. Kilminster,³⁸ D.H. Kim,²⁷ H.S. Kim,²⁷ J.E. Kim,²⁷ M.J. Kim,¹² M.S. Kim,²⁷ S.B. Kim,²⁷ S.H. Kim,⁵³ Y.K. Kim,¹³ M. Kirby,¹⁵ L. Kirsch,⁶ S. Klimentko,¹⁷ M. Klute,³¹ B. Knuteson,³¹ B.R. Ko,¹⁵ H. Kobayashi,⁵³ K. Kondo,⁵⁵ D.J. Kong,²⁷ J. Konigsberg,¹⁷ K. Kordas,¹⁸ A. Korytov,¹⁷ A.V. Kotwal,¹⁵ A. Kovalev,⁴³ J. Kraus,²³ I. Kravchenko,³¹ M. Kreps,²⁵ A. Kreymer,¹⁶ J. Kroll,⁴³ N. Krumnack,⁴ M. Kruse,¹⁵ V. Krutelyov,⁵¹ S. E. Kuhlmann,² Y. Kusakabe,⁵⁵ S. Kwang,¹³ A.T. Laasanen,⁴⁶ S. Lai,³² S. Lami,⁴⁴ S. Lammel,¹⁶ M. Lancaster,³⁰ R.L. Lander,⁷ K. Lannon,³⁸ A. Lath,⁵⁰ G. Latino,⁴⁴ I. Lazzizzera,⁴² C. Lecci,²⁵ T. LeCompte,² J. Lee,⁴⁷ J. Lee,²⁷ S.W. Lee,⁵¹ R. Lefèvre,³ N. Leonardo,³¹ S. Leone,⁴⁴ S. Levy,¹³ J.D. Lewis,¹⁶ K. Li,⁵⁸ C. Lin,⁵⁸ C.S. Lin,¹⁶ M. Lindgren,¹⁶ E. Lipelis,⁹ T.M. Liss,²³ A. Lister,¹⁹ D.O. Litvintsev,¹⁶ T. Liu,¹⁶ Y. Liu,¹⁹ N.S. Lockyer,⁴³ A. Loginov,³⁵ M. Loreti,⁴² P. Loverre,⁴⁹ R.-S. Lu,¹ D. Lucchesi,⁴² P. Lujan,²⁸ P. Lukens,¹⁶ G. Lungu,¹⁷ L. Lyons,⁴¹ J. Lys,²⁸ R. Lysak,¹ E. Lytken,⁴⁶ P. Mack,²⁵ D. MacQueen,³² R. Madrak,¹⁶ K. Maeshima,¹⁶ P. Maksimovic,²⁴ G. Manca,²⁹ F. Margaroli,⁵ R. Marginean,¹⁶ C. Marino,²³ A. Martin,⁵⁸ M. Martin,²⁴ V. Martin,³⁷ M. Martínez,³ T. Maruyama,⁵³ H. Matsunaga,⁵³ M.E. Mattson,⁵⁶ R. Mazini,³² P. Mazzanti,⁵ K.S. McFarland,⁴⁷ D. McGivern,³⁰ P. McIntyre,⁵¹ P. McNamara,⁵⁰ R. McNulty,²⁹ A. Mehta,²⁹ S. Menzemer,³¹ A. Menzione,⁴⁴ P. Merkel,⁴⁶ C. Mesropian,⁴⁸

A. Messina,⁴⁹ M. von der Mey,⁸ T. Miao,¹⁶ N. Miladinovic,⁶ J. Miles,³¹ R. Miller,³⁴ J.S. Miller,³³ C. Mills,¹⁰ M. Milnik,²⁵ R. Miquel,²⁸ S. Miscetti,¹⁸ G. Mitselmakher,¹⁷ A. Miyamoto,²⁶ N. Moggi,⁵ B. Mohr,⁸ R. Moore,¹⁶ M. Morello,⁴⁴ P. Movilla Fernandez,²⁸ J. Mülmenstädt,²⁸ A. Mukherjee,¹⁶ M. Mulhearn,³¹ Th. Muller,²⁵ R. Mumford,²⁴ P. Murat,¹⁶ J. Nachtman,¹⁶ S. Nahn,⁵⁸ I. Nakano,³⁹ A. Napier,⁵⁴ D. Naumov,³⁶ V. Necula,¹⁷ C. Neu,⁴³ M.S. Neubauer,⁹ J. Nielsen,²⁸ T. Nigmanov,⁴⁵ L. Nodulman,² O. Norniella,³ T. Ogawa,⁵⁵ S.H. Oh,¹⁵ Y.D. Oh,²⁷ T. Okusawa,⁴⁰ R. Oldeman,²⁹ R. Orava,²² K. Osterberg,²² C. Pagliarone,⁴⁴ E. Palencia,¹¹ R. Paoletti,⁴⁴ V. Papadimitriou,¹⁶ A. Papikonomou,²⁵ A.A. Paramonov,¹³ B. Parks,³⁸ S. Pashapour,³² J. Patrick,¹⁶ G. Paulette,⁵² M. Paulini,¹² C. Paus,³¹ D.E. Pellett,⁷ A. Penzo,⁵² T.J. Phillips,¹⁵ G. Piacentino,⁴⁴ J. Piedra,¹¹ K. Pitts,²³ C. Plager,⁸ L. Pondrom,⁵⁷ G. Pope,⁴⁵ X. Portell,³ O. Poukhov,¹⁴ N. Pounder,⁴¹ F. Prakoshyn,¹⁴ A. Pronko,¹⁶ J. Proudfoot,² F. Ptohos,¹⁸ G. Punzi,⁴⁴ J. Pursley,²⁴ J. Rademacker,⁴¹ A. Rahaman,⁴⁵ A. Rakitin,³¹ S. Rappoccio,²¹ F. Ratnikov,⁵⁰ B. Reisert,¹⁶ V. Rekovic,³⁶ N. van Remortel,²² P. Renton,⁴¹ M. Rescigno,⁴⁹ S. Richter,²⁵ F. Rimondi,⁵ K. Rinnert,²⁵ L. Ristori,⁴⁴ W.J. Robertson,¹⁵ A. Robson,²⁰ T. Rodrigo,¹¹ E. Rogers,²³ S. Rolli,⁵⁴ R. Roser,¹⁶ M. Rossi,⁵² R. Rossin,¹⁷ C. Rott,⁴⁶ A. Ruiz,¹¹ J. Russ,¹² V. Rusu,¹³ D. Ryan,⁵⁴ H. Saarikko,²² S. Sabik,³² A. Safoonov,⁷ W.K. Sakamoto,⁴⁷ G. Salamanna,⁴⁹ O. Salto,³ D. Saltzberg,⁸ C. Sanchez,³ L. Santi,⁵² S. Sarkar,⁴⁹ K. Sato,⁵³ P. Savard,³² A. Savoy-Navarro,¹⁶ T. Scheidle,²⁵ P. Schlabach,¹⁶ E.E. Schmidt,¹⁶ M.P. Schmidt,⁵⁸ M. Schmitt,³⁷ T. Schwarz,³³ L. Scodellaro,¹¹ A.L. Scott,¹⁰ A. Scribano,⁴⁴ F. Scuri,⁴⁴ A. Sedov,⁴⁶ S. Seidel,³⁶ Y. Seiya,⁴⁰ A. Semenov,¹⁴ F. Semeria,⁵ L. Sexton-Kennedy,¹⁶ I. Sfiligoi,¹⁸ M.D. Shapiro,²⁸ T. Shears,²⁹ P.F. Shepard,⁴⁵ D. Sherman,²¹ M. Shimojima,⁵³ M. Shochet,¹³ Y. Shon,⁵⁷ I. Shreyber,³⁵ A. Sidoti,⁴⁴ A. Sill,¹⁶ P. Sinervo,³² A. Sisakyan,¹⁴ J. Sjolin,⁴¹ A. Skiba,²⁵ A.J. Slaughter,¹⁶ K. Sliwa,⁵⁴ D. Smirnov,³⁶ J. R. Smith,⁷ F.D. Snider,¹⁶ R. Snihur,³² M. Soderberg,³³ A. Soha,⁷ S. Somalwar,⁵⁰ V. Sorin,³⁴ J. Spalding,¹⁶ F. Spinella,⁴⁴ P. Squillacioti,⁴⁴ M. Stanitzki,⁵⁸ A. Staveris-Polykalas,⁴⁴ R. St. Denis,²⁰ B. Stelzer,⁸ O. Stelzer-Chilton,³² D. Stentz,³⁷ J. Strologas,³⁶ D. Stuart,¹⁰ J.S. Suh,²⁷ A. Sukhanov,¹⁷ K. Sumorok,³¹ H. Sun,⁵⁴ T. Suzuki,⁵³ A. Taffard,²³ R. Tafirout,³² R. Takashima,³⁹ Y. Takeuchi,⁵³ K. Takikawa,⁵³ M. Tanaka,² R. Tanaka,³⁹ M. Tecchio,³³ P.K. Teng,¹ K. Terashi,⁴⁸ S. Tether,³¹ J. Thom,¹⁶ A.S. Thompson,²⁰ E. Thomson,⁴³ P. Tipton,⁴⁷ V. Tiwari,¹² S. Tkaczyk,¹⁶ D. Toback,⁵¹ K. Tollefson,³⁴ T. Tomura,⁵³ D. Tonelli,⁴⁴ M. Tönnesmann,³⁴ S. Torre,⁴⁴ D. Torretta,¹⁶ S. Tourneur,¹⁶ W. Trischuk,³² R. Tsuchiya,⁵⁵ S. Tsuno,³⁹ N. Turini,⁴⁴ F. Ukegawa,⁵³ T. Unverhau,²⁰ S. Uozumi,⁵³ D. Usynin,⁴³ L. Vacavant,²⁸ A. Vaiciulis,⁴⁷ S. Vallecorsa,¹⁹ A. Varganov,³³ E. Vataga,³⁶ G. Velev,¹⁶ G. Veramendi,²³ V. Veszprenyi,⁴⁶ T. Vickey,²³ R. Vidal,¹⁶ I. Vila,¹¹ R. Vilar,¹¹ I. Vollrath,³² I. Volobouev,²⁸ F. Würthwein,⁹ P. Wagner,⁵¹ R. G. Wagner,² R.L. Wagner,¹⁶ W. Wagner,²⁵ R. Wallny,⁸ T. Walter,²⁵ Z. Wan,⁵⁰ M.J. Wang,¹ S.M. Wang,¹⁷ A. Warburton,³² B. Ward,²⁰ S. Waschke,²⁰ D. Waters,³⁰ T. Watts,⁵⁰ M. Weber,²⁸ W.C. Wester III,¹⁶ B. Whitehouse,⁵⁴ D. Whiteson,⁴³ A.B. Wicklund,² E. Wicklund,¹⁶ H.H. Williams,⁴³ P. Wilson,¹⁶ B.L. Winer,³⁸ P. Wittich,⁴³ S. Wolbers,¹⁶ C. Wolfe,¹³ S. Worm,⁵⁰ T. Wright,³³ X. Wu,¹⁹ S.M. Wynne,²⁹ A. Yagil,¹⁶ K. Yamamoto,⁴⁰ J. Yamaoka,⁵⁰ Y. Yamashita,³⁹ C. Yang,⁵⁸ U.K. Yang,¹³ W.M. Yao,²⁸ G.P. Yeh,¹⁶ J. Yoh,¹⁶ K. Yorita,¹³ T. Yoshida,⁴⁰ I. Yu,²⁷ S.S. Yu,⁴³ J.C. Yun,¹⁶ L. Zanello,⁴⁹ A. Zanetti,⁵² I. Zaw,²¹ F. Zetti,⁴⁴ X. Zhang,²³ J. Zhou,⁵⁰ and S. Zucchelli⁵

(CDF Collaboration)

¹*Institute of Physics, Academia Sinica, Taipei, Taiwan 11529, Republic of China*

²*Argonne National Laboratory, Argonne, Illinois 60439*

³*Institut de Fisica d'Altes Energies, Universitat Autònoma de Barcelona, E-08193, Bellaterra (Barcelona), Spain*

⁴*Baylor University, Waco, Texas 76798*

⁵*Istituto Nazionale di Fisica Nucleare, University of Bologna, I-40127 Bologna, Italy*

⁶*Brandeis University, Waltham, Massachusetts 02254*

⁷*University of California, Davis, Davis, California 95616*

⁸*University of California, Los Angeles, Los Angeles, California 90024*

⁹*University of California, San Diego, La Jolla, California 92093*

¹⁰*University of California, Santa Barbara, Santa Barbara, California 93106*

¹¹*Instituto de Fisica de Cantabria, CSIC-University of Cantabria, 39005 Santander, Spain*

¹²*Carnegie Mellon University, Pittsburgh, PA 15213*

¹³*Enrico Fermi Institute, University of Chicago, Chicago, Illinois 60637*

¹⁴*Joint Institute for Nuclear Research, RU-141980 Dubna, Russia*

¹⁵*Duke University, Durham, North Carolina 27708*

¹⁶*Fermi National Accelerator Laboratory, Batavia, Illinois 60510*

¹⁷*University of Florida, Gainesville, Florida 32611*

¹⁸*Laboratori Nazionali di Frascati, Istituto Nazionale di Fisica Nucleare, I-00044 Frascati, Italy*

¹⁹*University of Geneva, CH-1211 Geneva 4, Switzerland*

- ²⁰Glasgow University, Glasgow G12 8QQ, United Kingdom
²¹Harvard University, Cambridge, Massachusetts 02138
²²Division of High Energy Physics, Department of Physics,
 University of Helsinki and Helsinki Institute of Physics, FIN-00014, Helsinki, Finland
²³University of Illinois, Urbana, Illinois 61801
²⁴The Johns Hopkins University, Baltimore, Maryland 21218
²⁵Institut für Experimentelle Kernphysik, Universität Karlsruhe, 76128 Karlsruhe, Germany
²⁶High Energy Accelerator Research Organization (KEK), Tsukuba, Ibaraki 305, Japan
²⁷Center for High Energy Physics: Kyungpook National University, Taegu 702-701; Seoul National University,
 Seoul 151-742; and SungKyunKwan University, Suwon 440-746; Korea
²⁸Ernest Orlando Lawrence Berkeley National Laboratory, Berkeley, California 94720
²⁹University of Liverpool, Liverpool L69 7ZE, United Kingdom
³⁰University College London, London WC1E 6BT, United Kingdom
³¹Massachusetts Institute of Technology, Cambridge, Massachusetts 02139
³²Institute of Particle Physics: McGill University, Montréal,
 Canada H3A 2T8; and University of Toronto, Toronto, Canada M5S 1A7
³³University of Michigan, Ann Arbor, Michigan 48109
³⁴Michigan State University, East Lansing, Michigan 48824
³⁵Institution for Theoretical and Experimental Physics, ITEP, Moscow 117259, Russia
³⁶University of New Mexico, Albuquerque, New Mexico 87131
³⁷Northwestern University, Evanston, Illinois 60208
³⁸The Ohio State University, Columbus, Ohio 43210
³⁹Okayama University, Okayama 700-8530, Japan
⁴⁰Osaka City University, Osaka 588, Japan
⁴¹University of Oxford, Oxford OX1 3RH, United Kingdom
⁴²University of Padova, Istituto Nazionale di Fisica Nucleare,
 Sezione di Padova-Trento, I-35131 Padova, Italy
⁴³University of Pennsylvania, Philadelphia, Pennsylvania 19104
⁴⁴Istituto Nazionale di Fisica Nucleare Pisa, Universities of Pisa,
 Siena and Scuola Normale Superiore, I-56127 Pisa, Italy
⁴⁵University of Pittsburgh, Pittsburgh, Pennsylvania 15260
⁴⁶Purdue University, West Lafayette, Indiana 47907
⁴⁷University of Rochester, Rochester, New York 14627
⁴⁸The Rockefeller University, New York, New York 10021
⁴⁹Istituto Nazionale di Fisica Nucleare, Sezione di Roma 1,
 University of Rome "La Sapienza," I-00185 Roma, Italy
⁵⁰Rutgers University, Piscataway, New Jersey 08855
⁵¹Texas A&M University, College Station, Texas 77843
⁵²Istituto Nazionale di Fisica Nucleare, University of Trieste/ Udine, Italy
⁵³University of Tsukuba, Tsukuba, Ibaraki 305, Japan
⁵⁴Tufts University, Medford, Massachusetts 02155
⁵⁵Waseda University, Tokyo 169, Japan
⁵⁶Wayne State University, Detroit, Michigan 48201
⁵⁷University of Wisconsin, Madison, Wisconsin 53706
⁵⁸Yale University, New Haven, Connecticut 06520

We present a measurement of the $t\bar{t}$ production cross section in $p\bar{p}$ collisions at $\sqrt{s} = 1.96$ TeV which uses events with an inclusive signature of significant missing transverse energy and jets. This is the first measurement which makes no explicit lepton identification requirements, so that sensitivity to $W \rightarrow \tau\nu$ decays is maintained. Heavy flavor jets from top quark decay are identified with a secondary vertex tagging algorithm. From 311 pb⁻¹ of data collected by the Collider Detector at Fermilab we measure a production cross section of $5.8 \pm 1.2(\text{stat.})^{+0.9}_{-0.7}(\text{syst.})$ pb for a top quark mass of 178 GeV/c², in agreement with previous determinations and standard model predictions.

PACS numbers: 13.85.Ni, 14.65.Ha

At the Tevatron $p\bar{p}$ collider top quarks are produced mainly in pairs through quark-antiquark annihilation and gluon-gluon fusion processes. In the standard model (SM) the calculated cross section for pair production is $6.1^{+0.6}_{-0.8}$ pb [1] for a top mass of 178 GeV/c² [2], and varies linearly with a slope of -0.2 pb/GeV/c² with the

top quark mass in the range $170 \text{ GeV}/c^2 < m_t < 190 \text{ GeV}/c^2$. Because the Cabibbo-Kobayashi-Maskawa matrix element V_{tb} is close to unity and m_t is large, the SM top quark decays to a W boson and a b quark almost 100% of the time. The final state of top quark pair production thus includes two W bosons and two b -quark jets.

When only one W decays leptonically, the $t\bar{t}$ event typically contains a charged lepton, missing transverse energy from the undetected neutrino, and four high transverse energy jets, two of which originate from b quarks [3]. Previous cross section analyses [4, 5, 6] select this distinct $t\bar{t}$ signature by requiring well-identified leptons (e , μ) with high transverse momentum. In this Letter we describe a $t\bar{t}$ production cross section measurement which is sensitive to leptonic W decays regardless of the lepton type, and has a sizable acceptance to τ decays of the W boson. The direct identification of τ from $W \rightarrow \tau\nu$ decays suffers from a very low efficiency, thus our measurement, using data collected by a multijet trigger, selects top decays by inclusively requiring a high- p_T neutrino signature rather than charged lepton identification. Events with well-identified high- p_T electrons or muons are explicitly vetoed in order to avoid statistical overlap and provide complementary results with respect to lepton-based measurements.

Results reported in this Letter are obtained from 311 pb $^{-1}$ of data from $p\bar{p}$ collisions at $\sqrt{s} = 1.96$ TeV recorded by the Collider Detector at Fermilab (CDF II). The CDF II detector has been described in detail elsewhere [7]. It consists of a magnetic spectrometer surrounded by calorimeter systems and muon chambers. The momenta of charged particles are measured up to a pseudorapidity of $|\eta| = 1.0$ in the central tracking chamber, which is inside a 1.4 T superconducting solenoidal magnet. Microstrip silicon vertex detectors, located immediately outside the beampipe, provide precise track reconstruction useful for vertexing and extend the $|\eta|$ coverage of the tracking system up to $|\eta| = 2.0$. Electromagnetic and hadronic sampling calorimeters, arranged in a projective-tower geometry, surround the tracking systems and measure the energy and direction of electrons, photons, and jets, providing good hermeticity in the pseudorapidity range $|\eta| < 3.6$. In addition, the calorimeter system allows the detection of high- p_T neutrinos by the measurement of the missing transverse energy, \cancel{E}_T [3]. Muon systems reside outside the calorimeters and consist of layers of drift chambers which allow the reconstruction of track segments for penetrating particles. The beam luminosity is determined using gas Cherenkov counters (CLC) located in the region $3.7 < |\eta| < 4.7$ which measure the average number of inelastic $p\bar{p}$ collisions per bunch crossing. The uncertainty on the luminosity measurement, due to CLC acceptance and theoretical uncertainties on the total inelastic $p\bar{p}$ cross section, is 6% [8].

The data sample used in this analysis is collected by a multijet trigger which requires four or more $E_T \geq 15$ GeV clusters of contiguous calorimeter towers, and a total transverse energy clustered in the calorimeter of $\sum E_T \geq 125$ GeV. The initial data sample consists of 4.2 million events. The understanding of signal acceptances and efficiencies relies on a detailed simulation of the pro-

duction processes and the detector response. Inclusively decaying $t\bar{t}$ events, assuming a top quark mass of 178 GeV/c 2 , are simulated using PYTHIA v6.2 [9] and HERWIG v6.5 [10] generators in conjunction with the CTEQ5L [11] parton distribution functions, QQV9.1 [12] for the modeling of b and c hadron decays, and a full simulation of the CDF II detector. Jets are identified as groups of calorimeter tower energy deposits which fall within a cone of radius $\Delta R = \sqrt{\Delta\phi^2 + \Delta\eta^2} \leq 0.4$. Jet energies, after the absolute energy scale setting, are corrected for calorimeter non-linearity, losses in the gap between towers, and multiple interactions [13].

The $t\bar{t}$ signature used in the present study ($\cancel{E}_T + \text{jets}$) consists of large missing transverse energy, \cancel{E}_T , associated with the neutrino from the leptonic decay of a W boson, and jets. Since the \cancel{E}_T resolution, $\sigma(\cancel{E}_T)$, is observed to degrade as a function of the total transverse energy of the event, in the form $\sigma(\cancel{E}_T) \propto \sqrt{\sum E_T}$ [14], the missing E_T significance, defined by $\cancel{E}_T^{sig} = |\cancel{E}_T|/\sqrt{\sum E_T}$, is used for event selection. Besides the requirement of large \cancel{E}_T^{sig} , further background rejection can be achieved by exploiting \cancel{E}_T -related geometrical properties. The neutrino direction for $t\bar{t} \rightarrow \cancel{E}_T + \text{jets}$ events is in general uncorrelated with the jet directions in the transverse plane. On the contrary, background events for which the \cancel{E}_T is mainly due to jet energy mis-measurement or to b -quark semileptonic decays are more likely to have \cancel{E}_T aligned with a jet direction. The minimum $\Delta\phi$ difference between the \cancel{E}_T and any jet in the event, $\min \Delta\phi(\cancel{E}_T, \text{jets})$, is used as an analysis cut. Events containing identified high- p_T electrons or muons, as defined in [5], are removed, in order to increase the relative contribution of $W \rightarrow \tau\nu$ decays and to provide a statistical independent sample with respect to other lepton+jets cross section analyses.

To reject events with only light quark or gluon jets, we require at least one jet to be identified as originating from a b -quark. The presence of b -jets (“tags”) is established by the identification of secondary decay vertices using the SECVTX algorithm [5]. An optimization procedure on the cross section measurement sets $N_{jet}(E_T \geq 15 \text{ GeV}; |\eta| \leq 2.0) \geq 4$, $\cancel{E}_T^{sig} \geq 4.0 \text{ GeV}^{1/2}$, and $\min \Delta\phi(\cancel{E}_T, \text{jets}) \geq 0.4 \text{ rad}$ as the best kinematical selection cuts. After these requirements the data sample is reduced to 597 events with an expected pre-tag signal to background ratio $S/B \sim 1/5$.

Background events with b -tags arise from QCD heavy flavor production, electroweak production of W bosons associated with heavy flavor jets, and from false identification by the SECVTX algorithm. The overall amount of background b -tags is estimated from the multijet sample by applying a parametrization of the per-jet tagging probability. The tagging probability is calculated using $\sim 879,000$ multijet data events with exactly three jets having $E_T \geq 15$ GeV and $|\eta| \leq 2.0$. It is parametrized

on a per-jet basis as a function of the jet E_T , track multiplicity, and the projection of the \vec{E}_T along the jet direction, defined by $E_T^{proj} = \vec{E}_T \cdot \cos \Delta\phi(\vec{E}_T, jet)$. The $t\bar{t}$ contamination in this control sample is negligible. The jet b -tagging rate, calculated as the ratio between the number of b -tagged jets and the number of jets with at least two good tracks with hits in the silicon detector, is shown in Fig. 1. The E_T^{proj} parametrization accounts for background b -tags from $b\bar{b}$ production processes, whose b -tag rate is enhanced at high positive values of the E_T^{proj} due to the correlation of \vec{E}_T and b -jet direction in the case of a semileptonic b -quark decay. The extrapolation of the 3-jet b -tag rate to higher jet multiplicity events is checked by comparing the predicted and observed b -tag rates as a function of the number of jets in the multijet sample without the kinematical selection on E_T^{sig} and $\min \Delta\phi(\vec{E}_T, jets)$, as shown in Fig. 2(a). The capability of the parametrization to track possible sample composition changes introduced by the kinematical selection is proven by constructing the ratio of observed over expected b -tags in two separate control samples of multijet data, depleted of signal contaminations, as shown in Fig. 2(b) and Fig. 2(c), respectively. The first control sample is defined by $E_T^{sig} \leq 3.0 \text{ GeV}^{1/2}$, $\min \Delta\phi(\vec{E}_T, jets) \geq 0.3 \text{ rad}$; the second as $E_T^{sig} \geq 3.0 \text{ GeV}^{1/2}$,

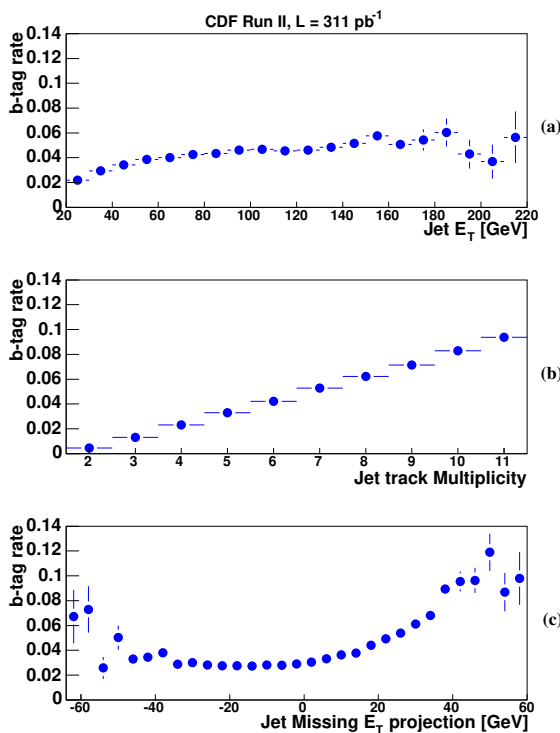


FIG. 1: Tagging rate probability parametrization in the multijet sample as a function of jet E_T (a), track multiplicity (b), and missing E_T projection (c).

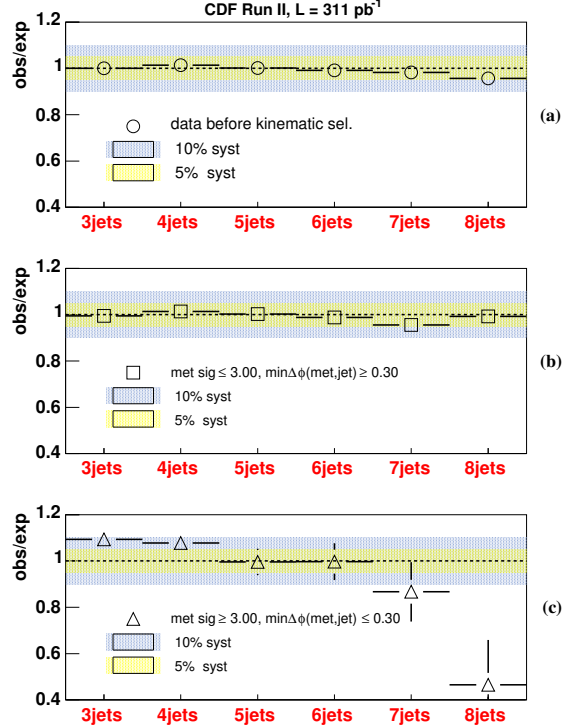


FIG. 2: Ratio of observed to expected b -tags as a function of the number of jets in the data before the optimized kinematical selection on E_T^{sig} and $\min \Delta\phi(\vec{E}_T, jets)$ (a), and in control samples: $E_T^{sig} \leq 3.0 \text{ GeV}^{1/2}$, $\min \Delta\phi(\vec{E}_T, jets) \geq 0.3 \text{ rad}$ (b); and $E_T^{sig} \geq 3.0 \text{ GeV}^{1/2}$, $\min \Delta\phi(\vec{E}_T, jets) \leq 0.3 \text{ rad}$ (c).

$\text{GeV}^{1/2}$, $\min \Delta\phi(\vec{E}_T, jets) \leq 0.3 \text{ rad}$. The b -tag rate parametrization is found to predict the non- $t\bar{t}$ background within 10%, which is thus adopted as systematic uncertainty on the background prediction. Additional checks, using low jet multiplicity events from leptonic W data samples, show agreement between observed and predicted b -tags within the quoted uncertainty.

The sample selected with the optimized kinematical requirements described above and the requirement of at least one b -tagged jet consists of 106 events, containing a total of 127 b -tagged jets. The number of b -tagged jets yielded by background processes in that sample is expected to be $N_{exp} = 67.4 \pm 2.7 \pm 6.7$. The first uncertainty contribution is due to the limited number of events in the 3-jet sample used for the tagging rate parametrization, while the second contribution is the 10% systematic uncertainty on the b -tag rate parameterization discussed above (Fig. 2). The N_{exp} value needs to be corrected, to $N'_{exp} = 57.4 \pm 8.1$, to account for the $t\bar{t}$ signal contamination in the pre-tagging data sample. Table I summarizes the number of b -tagged jets expected from each $t\bar{t}$ decay mode satisfying the kinematical and ≥ 1 b -tag requirements, as well as the predicted and observed b -tags in the selected data sample as a function of the jet multiplicity

TABLE I: Number of b -tagged jets expected from $t\bar{t}$ production using $\sigma(t\bar{t}) = 6.1 \text{ pb}$ ($m_t = 178 \text{ GeV}/c^2$), predicted by the tagging rate parametrization, and observed in the selected sample, as a function of the jet multiplicity. The total uncertainty on the number of predicted background b -tags is the sum in quadrature of the statistical uncertainty and of a 10% systematic uncertainty. The number of background b -tags corrected for the $t\bar{t}$ contamination in the pre-tagging data sample is also provided for the signal region. Uncertainties on signal contributions are statistical only.

Number of jets	3	4	5	≥ 6
$t\bar{t} \rightarrow ee$	0.08 ± 0.01	0.41 ± 0.03	0.18 ± 0.02	0.04 ± 0.01
$t\bar{t} \rightarrow e\mu$	0.06 ± 0.01	0.29 ± 0.02	0.11 ± 0.01	0.05 ± 0.01
$t\bar{t} \rightarrow \mu\mu$	0.01 ± 0.01	0.05 ± 0.01	0.01 ± 0.01	0.01 ± 0.01
$t\bar{t} \rightarrow e\tau$	0.11 ± 0.01	0.93 ± 0.04	0.38 ± 0.03	0.15 ± 0.02
$t\bar{t} \rightarrow \mu\tau$	0.05 ± 0.01	0.29 ± 0.02	0.15 ± 0.02	0.06 ± 0.01
$t\bar{t} \rightarrow \tau\tau$	0.06 ± 0.01	0.58 ± 0.03	0.26 ± 0.02	0.05 ± 0.01
$t\bar{t} \rightarrow e + jets$	0.68 ± 0.04	6.61 ± 0.11	8.70 ± 0.13	4.25 ± 0.09
$t\bar{t} \rightarrow \mu + jets$	1.07 ± 0.04	11.92 ± 0.15	6.56 ± 0.11	2.47 ± 0.07
$t\bar{t} \rightarrow \tau + jets$	1.00 ± 0.04	10.98 ± 0.14	11.71 ± 0.15	5.53 ± 0.10
$t\bar{t} \rightarrow jets$	0.01 ± 0.01	0.09 ± 0.01	0.14 ± 0.02	0.22 ± 0.02
$t\bar{t} \rightarrow X$	3.13 ± 0.08	32.15 ± 0.24	28.14 ± 0.23	12.83 ± 0.15
Background b -tagged jets	32.68 ± 3.46	37.53 ± 4.14	21.44 ± 2.76	8.47 ± 1.40
Corrected background b -tagged jets	—	33.14 ± 4.01	17.58 ± 2.85	6.71 ± 2.78
Observed b -tagged jets	31	53	55	19

of the events. In Table I, the numbers of b -tags from events with only three jets are provided as a cross-check of the background. The excess in the number of b -tags, for $N(jet) \geq 4$, is ascribed to top pair production. Final states with $W \rightarrow \tau\nu$ decays account for $\sim 44\%$ of the signal acceptance.

In order to further establish the $t\bar{t}$ signal in the selected data we perform binned likelihood fits to kinematical distributions. The stability of the fitting technique is checked using simulations with known signal fractions. We fit \cancel{E}_T and $\Delta\phi(\cancel{E}_T, \text{tagged jet})$ data distributions to the sum of a $t\bar{t}$ and a background template. The former is obtained from Monte Carlo $t\bar{t}$ inclusive events; the latter is derived from the tagging rate parametrization applied to the data. Results are displayed in Fig. 3. The fitted $t\bar{t}$ components in the selected data ($68 \pm 12\%$ and $44 \pm 12\%$ for the \cancel{E}_T and $\Delta\phi(\cancel{E}_T, \text{tagged jet})$ fits respectively) are in agreement with the overall prediction calculated from b -tag counting, before any correction to account for the $t\bar{t}$ contamination in the pre-tagging data sample ($47 \pm 5\%$ determined comparing the number of expected and observed b -tags, for $N_{jet} \geq 4$, in Table I).

The efficiency of the trigger, the kinematical selection, and the b -tagging algorithm, are evaluated using inclusive $t\bar{t}$ Monte Carlo events. The combined efficiency of trigger and kinematical selection amounts to $\epsilon_{kin} = 4.88\% \pm 0.43\%$ for a top mass of $m_t = 178 \text{ GeV}/c^2$, where the dominant uncertainty is determined by the comparison of PYTHIA and HERWIG generators. Other sources of systematic uncertainty are evaluated by varying Monte Carlo generation settings with respect to the default values, and by applying systematic variations of

TABLE II: Relevant sources of systematic uncertainty.

Source	relative error
ϵ_{kin} systematics	
Generator dependence	8.2 %
Trigger acceptance	2.0 %
ISR/FSR	2.0 %
PDFs	1.6 %
Jet Energy Scale	1.5 %
Others	
Background prediction method	10.0 %
Luminosity measurement	6.0 %
ϵ_{tag}^{ave} (SECVTX scale factor)	5.8 %

the jet correction factors; the trigger acceptance uncertainty is determined by comparing trigger turn-on curves between Monte Carlo and data events (Table II). The average number of b -tags per $t\bar{t}$ event is found to be $\epsilon_{tag}^{ave} = 0.789 \pm 0.046$, and it is corrected according to the Monte Carlo SECVTX efficiency scale factor to reproduce the data b -tagging efficiency [5].

The cross section is calculated with a Poisson likelihood function in which the maximum likelihood solution for $\sigma(t\bar{t})$ is given by: $\sigma(t\bar{t}) = \frac{N_{obs} - N'_{exp}}{\epsilon_{kin} \cdot \epsilon_{tag}^{ave} \cdot \mathcal{L}_{int}}$, where N_{obs} and N'_{exp} are the number of b -tagged jets observed and expected from background events by the tagging rate parametrization in the selected data, and \mathcal{L}_{int} is the integrated luminosity of the multijet data sample. The input parameters: \mathcal{L}_{int} , ϵ_{kin} , ϵ_{tag}^{ave} , and N'_{exp} are

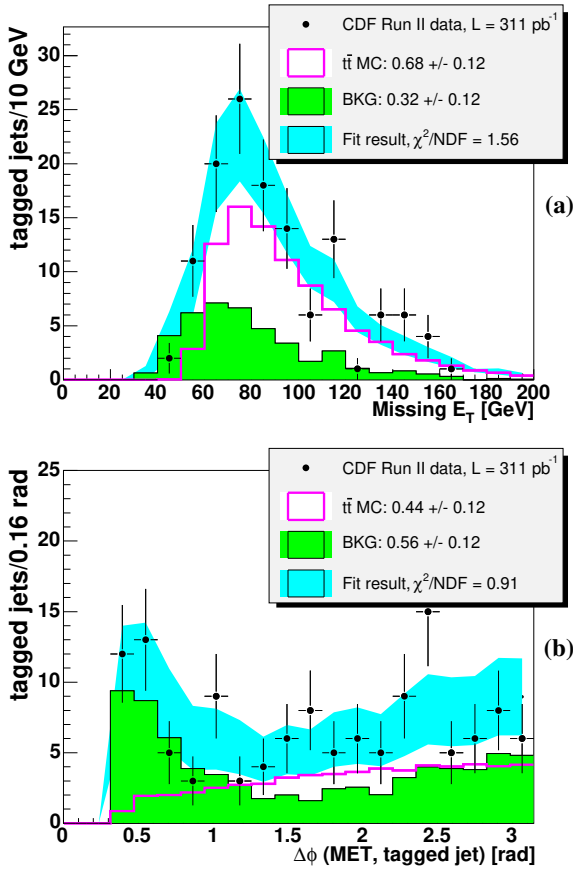


FIG. 3: \cancel{E}_T (a) and $\Delta\phi(\cancel{E}_T, \text{tagged jet})$ (b) distributions for data after kinematical selection and with at least one b -tagged jet. The data is fit to the sum of $t\bar{t}$ signal and background templates as described in the text.

subject to Gaussian constraints. With these input values we measure a top pair production cross section of $5.8 \pm 1.2(\text{stat.})^{+0.9}_{-0.7}(\text{syst.})$ pb. Additional samples of inclusive $t\bar{t}$ Monte Carlo events generated with different m_t values in the range [130, 230] GeV/ c^2 are used to compute the cross section measurement dependence on m_t . The cross section measurement changes by ± 0.05 pb for each ∓ 1 GeV/ c^2 change in the top quark mass from the initial value of 178 GeV/ c^2 . For instance, we measure $\sigma(t\bar{t}) = 6.0 \pm 1.2(\text{stat.})^{+0.9}_{-0.7}(\text{syst.})$ pb assuming a top quark mass of 175 GeV/ c^2 . The change is due to the varying signal selection efficiency with top quark mass.

In conclusion we report the first measurement of the top pair production cross section of $\sigma(t\bar{t}) = 5.8^{+1.5}_{-1.4}$ pb using an inclusive selection of $\cancel{E}_T + \text{jets } t\bar{t}$ decays. The result is complementary to other cross section analyses [4, 5, 6], maintains high sensitivity with respect to $W \rightarrow \tau\nu$ $t\bar{t}$ decays, and is in good agreement with SM calculations [1] and previous measurements.

We thank the Fermilab staff and the technical staffs of the participating institutions for their vital contribu-

tions. This work was supported by the U.S. Department of Energy and National Science Foundation; the Italian Istituto Nazionale di Fisica Nucleare; the Ministry of Education, Culture, Sports, Science and Technology of Japan; the Natural Sciences and Engineering Research Council of Canada; the National Science Council of the Republic of China; the Swiss National Science Foundation; the A.P. Sloan Foundation; the Bundesministerium für Bildung und Forschung, Germany; the Korean Science and Engineering Foundation and the Korean Research Foundation; the Particle Physics and Astronomy Research Council and the Royal Society, UK; the Russian Foundation for Basic Research; the Comisión Interministerial de Ciencia y Tecnología, Spain; in part by the European Community's Human Potential Programme under contract HPRN-CT-2002-00292; and by the Academy of Finland.

-
- [1] M. Cacciari, S. Frixione, M. L. Mangano, P. Nason, and G. Ridolfi, J. High Energy Phys. **0404** (2004) 068; N. Kidonakis and R. Vogt, Phys. Rev. D **68** (2003) 114014.
 - [2] CDF and DØ collaborations, hep-ex/0404010.
 - [3] The CDF II coordinate system uses θ and ϕ as the polar and azimuthal angles, respectively, defined with respect to the proton beam axis direction, z . The pseudorapidity η is defined as $\eta = -\ln[\tan(\theta/2)]$. The transverse momentum of a particle is $p_T = p \sin(\theta)$ and the transverse energy is defined as $E_T = E \sin(\theta)$. The missing transverse energy, \cancel{E}_T , is defined by $\cancel{E}_T = -\sum_i E_T^i \hat{\mathbf{n}}_i$, where the index i runs over all calorimeter towers with $|\eta| < 3.6$, and $\hat{\mathbf{n}}_i$ is a unit vector perpendicular to the beam axis and pointing at the i^{th} calorimeter tower.
 - [4] D. Acosta *et al.* (CDF Collaboration), Phys. Rev. D **72**, 032002 (2005); **71**, 072005 (2005).
 - [5] D. Acosta *et al.* (CDF Collaboration), Phys. Rev. D **71**, 052003 (2005);
 - [6] V. M. Abazov *et al.* (DØ Collaboration), Phys. Lett. B **626**, 35 (2005); **626**, 45 (2005); **626**, 55 (2005).
 - [7] D. Acosta *et al.* (CDF Collaboration), Phys. Rev. D **71**, 032001 (2005).
 - [8] D. Acosta *et al.*, Nucl. Instrum. Methods, A494, 57 (2002); S. Klimenko, J. Konigsberg, and T.M. Liss, FERMILAB-FN-0741 (2003).
 - [9] T. Sjostrand, P. Eden, C. Friberg, L. Lonnblad, G. Miu, S. Mrenna, and E. Norrbin, Comput. Phys. Commun. 135 (2001) 238.
 - [10] G. Marchesini, B.R. Webber, G. Abbiendi, I.G. Knowles, M.H. Seymour, and L. Stanco, Comput. Phys. Commun. 67 (1992) 465.
 - [11] J. Pumplin, D. R. Stump, J. Huston, H. L. Lai, P. Nadolsky, and W. K. Tung, J. High Energy Phys. **0207** (2002) 012.
 - [12] P. Avery, K. Read, and G. Trahern (1985), CLEO Report CSN-212 (unpublished).
 - [13] A. Bhatti *et al.*, hep-ex/0510047.
 - [14] F. Abe *et al.* (CDF Collaboration), Phys. Rev. D **50** (1994) 2966.